# APPENDIX AVAILABLE ON THE HEI WEB SITE

## Research Report 178

## National Particle Component Toxicity (NPACT) Initiative Report on Cardiovascular Effects

**Sverre Vedal et al.**

## Section 1: NPACT Epidemiologic Study of Components of Fine Particulate Matter and Cardiovascular Disease in the MESA and WHI-OS Cohorts

## Appendix C. Building and Validating the MESA Spatial and Spatiotemporal Models

Note: Appendices that are available only on the Web have been assigned letter identifiers that differ from the lettering in the original Investigators' Report. HEI has not changed the content of these documents, only their identifiers.

Appendix C was originally Appendix B

---

Correspondence may be addressed to Dr. Sverre Vedal, University of Washington, Department of Environmental and Occupational Health Sciences, Box 354695, 4225 Roosevelt Way NE, Suite 100, Seattle, WA 98105-6099; email: *svedal@uw.edu*.

Although this document was produced with partial funding by the United States Environmental Protection Agency under Assistance Award CR–83234701 to the Health Effects Institute, it has not been subjected to the Agency's peer and administrative review and therefore may not necessarily reflect the views of the Agency, and no official endorsement by it should be inferred. For the research funded under the National Particle Component Toxicity initiative, HEI received additional funds from the American Forest & Paper Association, American Iron and Steel Institute, American Petroleum Institute, ExxonMobil, and Public Service Electric and Gas. The contents of this document also have not been reviewed by private party institutions, including those that support the Health Effects Institute; therefore, it may not reflect the views or policies of these parties, and no endorsement by them should be inferred.

This document was reviewed by the HEI NPACT Review Panel but did not undergo the HEI scientific editing and production process.

## APPENDIX B: Building and Validating the MESA spatial and spatio-temporal models

- **Comparison of measurements between different monitoring networks**
- **MESA Air/NPACT data cleaning**
- **Prediction model for LA and NY**
- **Various approaches for the spatio-temporal model**
- **Estimated regression and variance parameters**
- **Calculation of temporally-adjusted $R^2$**

## Comparison of measurements between different monitoring networks

### *Data inconsistency between EPA AQS and MESA Air monitoring data*

The protocols to monitor, sample, and analyze filter samples differed across networks. Addressing the monitoring schedules first, Table 1 in Appendix B lists the number of monitoring sites located by monitoring network within the MESA Air regions. In contrast to the MESA Air fixed sites, all EPA monitoring sites operate every 3$^{rd}$ or 6$^{th}$ day. This means there are a maximum of 3 (for every 6$^{th}$ day measurement locations) or 5 (for every 3$^{rd}$ day measurement locations) observations available to compute the 2-week averages used in the spatio-temporal model. In all our previous spatio-temporal modeling of $PM_{2.5}$, we did not include sites operating under a 6-day monitoring schedule because there were too few available observations to reliably estimate a two-week average (Sampson 2011).

More significant discrepancies were caused by the sampling and analysis protocols. The CSN and IMPROVE networks adopted different methods to sample and analyze carbon data. (Recall also that MESA Air uses a protocol similar to the IMPROVE protocol for carbon data.) Given published results (Watson 2005) and further support from our own exploratory analyses, CSN carbon data acquired using the old method are not useful in our spatio-temporal model. Furthermore, the sampling protocols are also different because of different sampling equipment resulting in different air flows between the new CSN and in MESA Air/NPACT. Given these protocol differences, we decided it was essential to assess the degree of between-network consistency and only include the CSN and IMPROVE data in our spatio-temporal models if there was sufficient evidence of consistency. As summarized in the next section, we concluded the networks are not consistent enough to allow us to combine data across networks in a single model.

***Exploratory analysis to assess the appropriateness of including AQS data in the spatio-temporal model***

Our primary approach to determining what data to include in the spatio-temporal model was to compare measurements between networks at co-located sites. Appendix Figure B.1 shows the difference of log(EC) and log(OC) between pre- and post-method change at CSN sites. Note there are non-systematic differences between the methods (as evident by variation in the best fit lines across sites) and limited data in a 2-month time period when both methods were used. These features prevent the development of a reasonable calibration model. Appendix Figure B.2 shows that components measured by the new method at CSN sites are not comparable to those at co-located MESA Air fixed sites. Again there is variability in the best fit lines and degree of correlation across locations with the most consistency evident for sulfur. In addition, the CSN and MESA, using time series plots of log(EC) with overlaid smoothed trends for the same data used in Appendix Figure B.3, give further evidence of the non-comparability of even the new CSN measurements and our MESA Air measurements (similar results for other components not shown).Thus we concluded from our exploratory analysis results that there was a lack of consistency in the data across networks; this led us to decide to use MESA Air monitoring data only in our spatio-temporal modeling. The decision to utilize only the MESA Air data reduced substantially the amount of data available in fitting the spatio-temporal model for $PM_{2.5}$ components compared to other pollutants such as NOx (Appendix Table B.1.B)

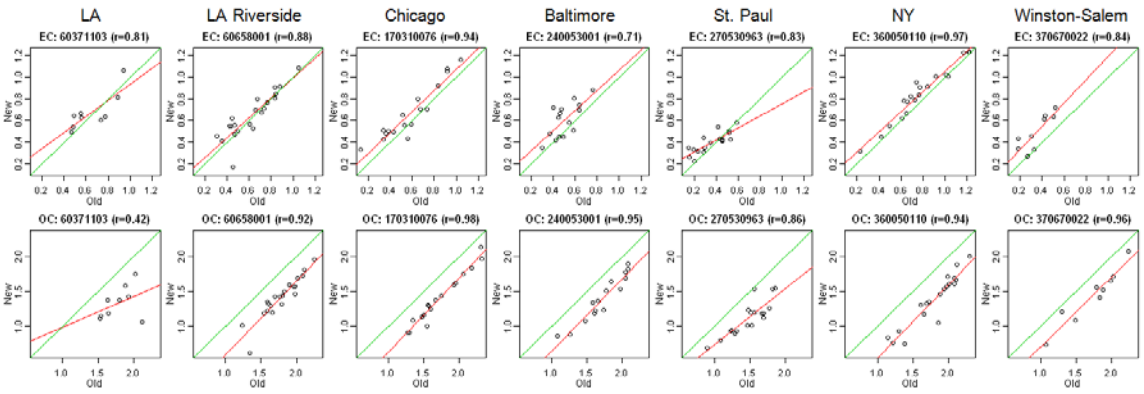


Best fit line, 45 degree line

Appendix Figure B.1. Scatter plots of log-transformed EC and OC measured by old and new protocols at 7 CSN sites in 6 MESA Air city areas during the overlapping 2 months from May through July in 2007

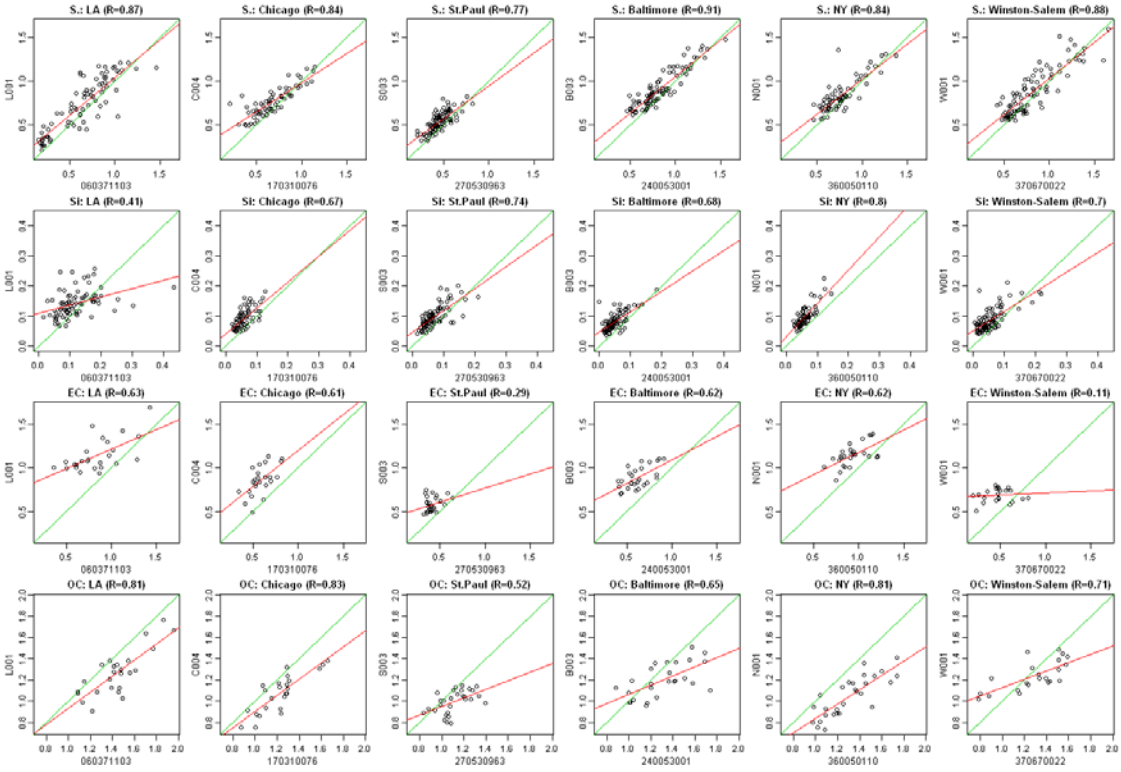


Best fit line, 45 degree line

Appendix Figure B.2. Scatter plots of log-transformed sulfur, silicon, EC, and OC measured by the IMPROVE-like method at co-located CSN and MESA Air fixed sites in 6 MESA AIR city areas

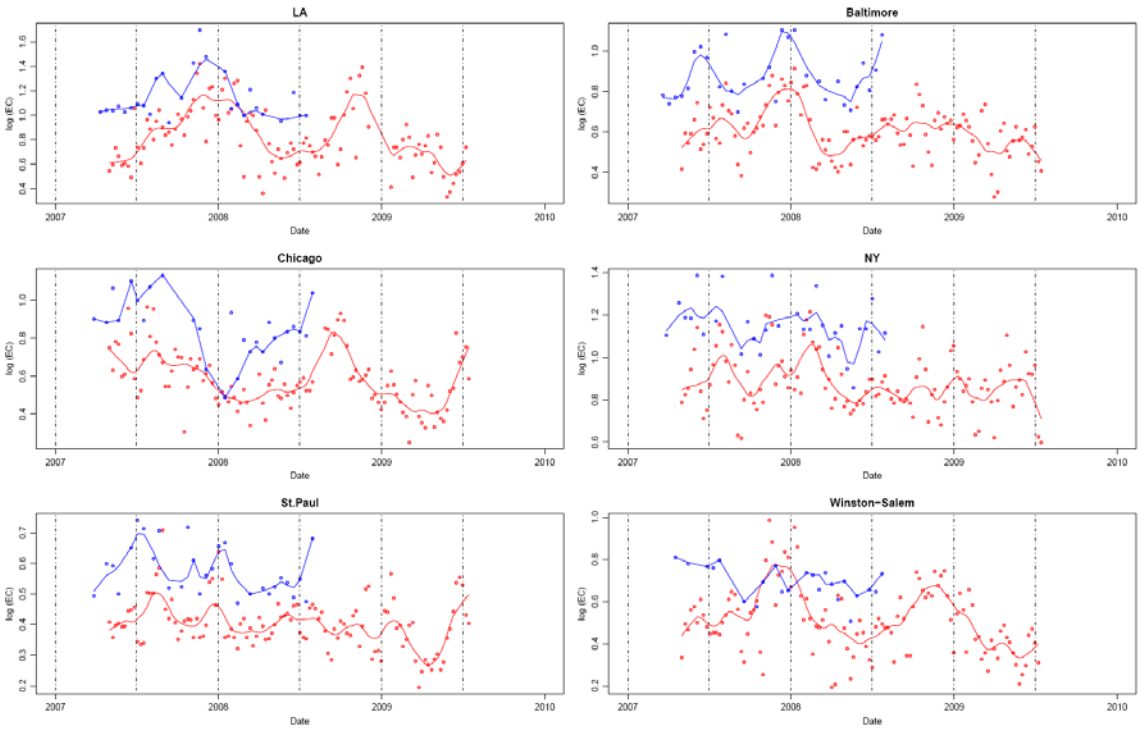


log(EC) at CSN sites; log(EC) at MESA Air fixed sites

Appendix Figure B.3. Time trends of log transformed EC measured by the IMPROVE-like method at co-located CSN and MESA Air fixed sites in 6 MESA AIR city areas

**MESA Air/NPACT data cleaning**

While the flags for source pollution and concentration did not invalidate samples, the flags for pump dysfunction affecting air flow did (MESA Air QAQC Committee Report). We decided to exclude measurements with pump flags when they were less than or greater than any non-flagged measurements. The extremely high silicon measurements were possibly due to greases of sampling devices and were also excluded. In addition, in order to prevent influential observations from affecting the model fitting and prediction, we used a conservative approach and removed all measurements we considered to be outliers. Outliers were defined temporally and spatially; values less than the first quartile minus 2.5 times interquartlie range or greater than the third quartile plus 2.5 times interquartlie range for a time-series of measurements in each fixed or all home sites by city (Appendix Figure B.8), and for spatially-distributed measurements across all sites at each time by city. In our preliminary analysis, we found that our estimated trends represented local trends of outliers instead of general seasonal trends. We also found that the predicted values were less correlated with the observed values when our model included outliers as compared to models that excluded outliers (Appendix Figure B.9 and B.10).

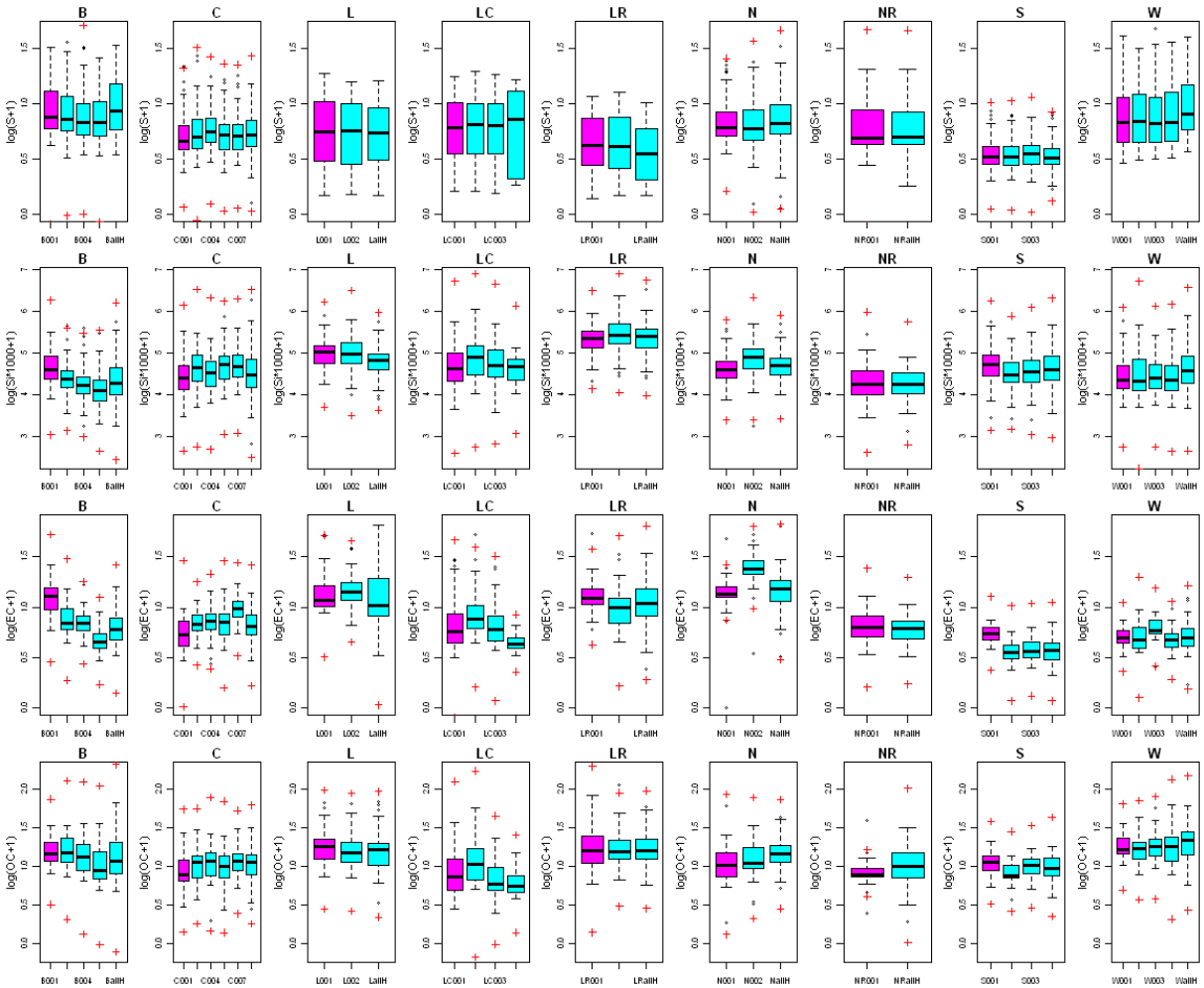

Appendix Figure B.8. Box plots and outliers of four components by fixed and home-outdoor sites in 6 MESA Air cities

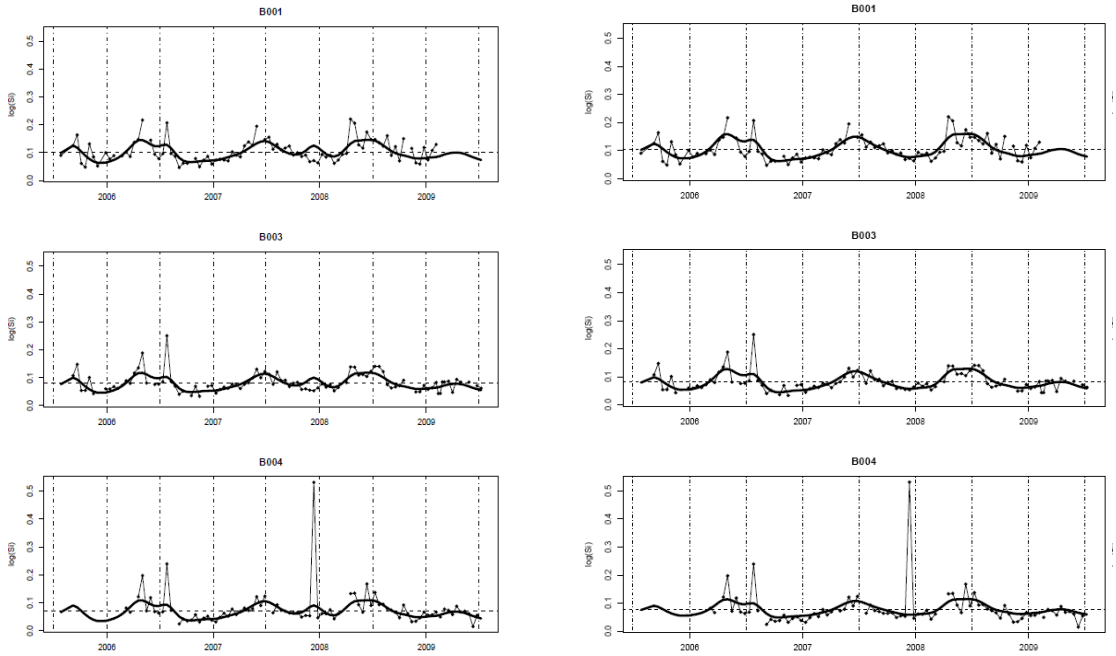


Appendix Figure B.9. Fitted temporal trends for silicon at three sites in Baltimore before and after excluding one outlier at B004

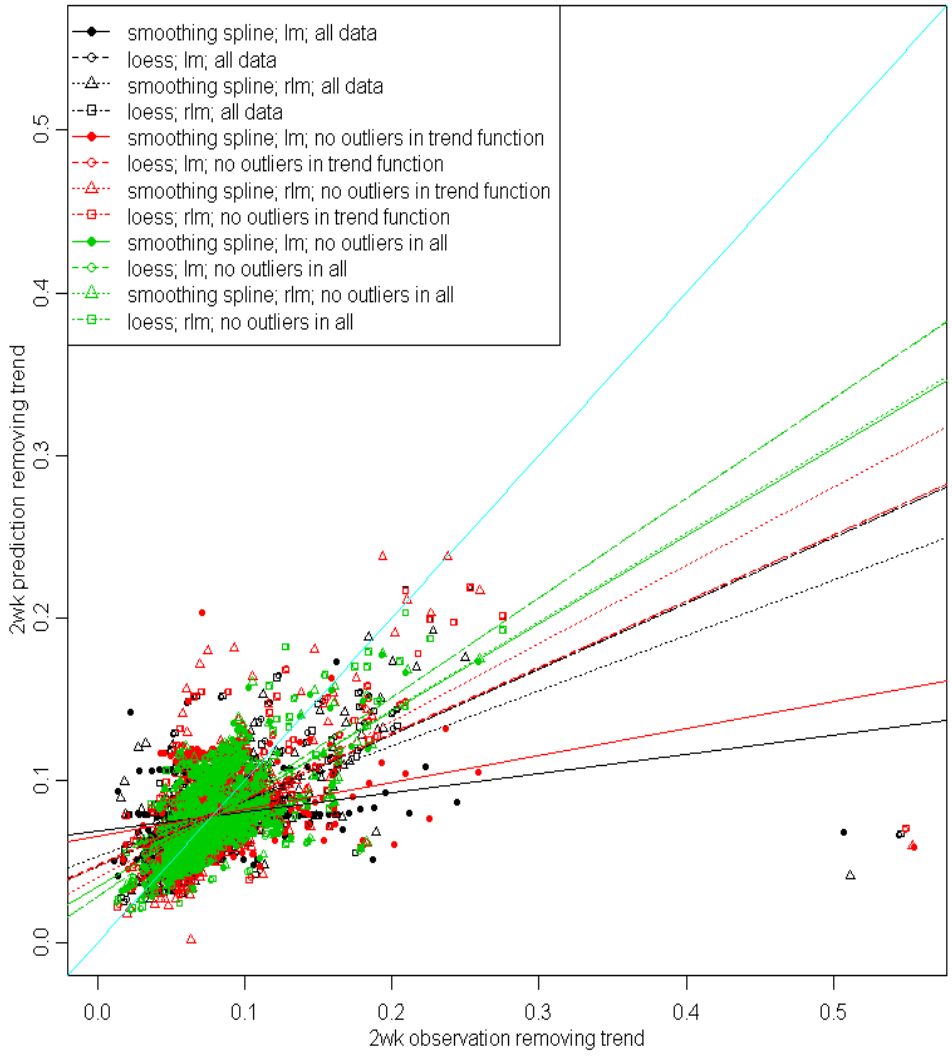


Appendix Figure B.10. Scatter plots of observed and predicted 2-week time-removed concentrations by different approaches dealing with outliers

Appendix Table B.1.A Main data processing procedure for geographic variables

| Procedure | Reason for exclusion or re-computation |
|---|---|
| 1. Drop population density | Less meaningful than absolute population |
| 2. Transform distance to roads (log10) and delete for smaller than 10 m | Higher effect in closer distance |
| 3. Compute distance to any road, and drop distance to a2 and a3 | Higher effect of A1 than A2 and A3 |
| 4. Merge a2 and a3 road buffers and remove the individual a2 and a3 | No difference between A2 and A3 in some cities |
| 5. Truncate distance to coast at 15 km instead of 25 km | Plausible effect of coast line within 15 km |
| 6. Compute distance to any port | Too few ports to consider size difference |
| 7. Drop covariates with less than 10 % of different values | Few different values for many land use variables |
| 8. Drop land use covariates within less than 300 m buffer | Less accuracy for small area |

Appendix Table B.1.B. Numbers of sites and samples for metal, carbon, and NOx data by monitor type and city

| City | Type | Metal | | Carbon | | NOx | |
|---|---|---|---|---|---|---|---|
| | | Site | Sample | Site | Sample | Site | Sample |
| Los Angeles | AQS | — | — | — | — | 27 | 5423 |
| | Snapshot | 0 | 0 | 0 | 0 | 252 | 611 |
| | Fixed | 7 | 515 | 7 | 143 | 7 | 599 |
| | Home | 113 | 175 | 116 | 77 | 120 | 217 |
| Chicago | AQS | — | — | — | — | 8 | 1472 |
| | Snapshot | 0 | 0 | 0 | 0 | 129 | 302 |
| | Fixed | 7 | 377 | 7 | 90 | 7 | 448 |
| | Home | 99 | 154 | 99 | 61 | 113 | 255 |
| Minneapolis-St. Paul | AQS | — | — | — | — | 5 | 810 |
| | Snapshot | 0 | 0 | 0 | 0 | 107 | 285 |
| | Fixed | 3 | 247 | 3 | 56 | 4 | 345 |
| | Home | 104 | 187 | 104 | 55 | 129 | 270 |
| Baltimore | AQS | — | — | — | — | 13 | 2371 |
| | Snapshot | 0 | 0 | 0 | 0 | 104 | 306 |
| | Fixed | 5 | 339 | 5 | 98 | 5 | 387 |
| | Home | 86 | 157 | 87 | 66 | 87 | 173 |
| New York | AQS | — | — | — | — | 17 | 2723 |
| | Snapshot | 0 | 0 | 0 | 0 | 157 | 409 |
| | Fixed | 3 | 187 | 3 | 75 | 3 | 246 |
| | Home | 107 | 191 | 107 | 73 | 119 | 244 |
| Winston-Salem | AQS | — | — | — | — | 3 | 569 |
| | Snapshot | 0 | 0 | 0 | 0 | 121 | 308 |
| | Fixed | 4 | 347 | 4 | 71 | 4 | 371 |
| | Home | 92 | 178 | 92 | 55 | 117 | 270 |

**Prediction model for LA and NY**

To predict $PM_{2.5}$ component concentrations at participant locations in central LA and NY, we examined whether or not there was any advantage to using the data and information obtained in LA Riverside and NY Rockland. We investigated three models: 1) both monitoring data in and GIS covariates selected from locations in the central area, 2) data from the combined area and covariates selected from only the central area, and 3) both data in and covariates selected from the combined area. The best models were determined based on cross-validation statistics giving the highest temporally-adjusted $R^2$. The selected models for four components were 1) except for OC with 3) in LA and 1) in NY, respectively (Appendix Table B.2). We also explored the addition of an indicator variable for the central vs. other areas, but temporally-adjusted $R^2$ was lower. These selected approaches were used for the final prediction model of the four components.

Appendix Table B.2. Temporally-adjusted $R^2$ of different approaches for combined areas in LA and NY

| City | LA | | | | | | NY | | | | | |
|---|---|---|---|---|---|---|---|---|---|---|---|---|
| Area# | 1) | | 2) | | 3) | | 1) | | 2) | | 3) | |
| Temporally -adjusted $R^2$ | Trend* | Average+ | Trend | Average | Trend | Average | Trend | Average | Trend | Average | Trend | Average |
| Sulfur | **0.84** | **0.46** | 0.83 | 0.46 | 0.83 | 0.48 | **0.19** | **0.00** | 0.19 | 0.00 | 0.14 | 0.00 |
| Silicon | **0.65** | **0.46** | 0.56 | 0.36 | 0.57 | 0.35 | **0.29** | **0.39** | 0.30 | 0.43 | 0.28 | 0.41 |
| EC | **0.67** | **0.64** | 0.53 | 0.44 | 0.51 | 0.42 | **0.57** | **0.49** | 0.52 | 0.46 | 0.48 | 0.41 |
| OC | 0.40 | 0.29 | 0.40 | 0.24 | **0.53** | **0.40** | **0.58** | **0.47** | 0.07 | 0.00 | 0.31 | 0.26 |

* Adjusted temporal trend was defined by unsmoothed temporal trend estimated using measurements across fixed sites

+ Adjusted temporal trend was defined by mean of measurements across fixed sites at each time

# Bold for selected areas based on the highest temporally-adjusted $R^2$

**Various approaches for the spatio-temporal model**

We considered 18 different approaches of the spatio-temporal model depending on the inclusion of spatial correlation for the long-term mean and the spatio-temporal residuals and the inclusion of measurement error for the long-term mean and the temporal trend coefficient by each component and city (Appendix Table B.3). We selected models with spatial correlation structure, when estimated range and partial sill parameters were reasonably large and stable based on their 95% confidence intervals. Then, the final models shown in Appendix Table B.4 were chosen using the highest temporally-adjusted $R^2$ in cross-validation. In addition to the full spatio-temporal model approach, we also explored the simplified version by removing the temporal trend and modeling trend-removed 2-week concentrations in order to avoid estimating site-specific temporal trends and to reduce the number of parameters in the model given the limited data. Because the full spatio-temporal model approach gave more stable parameter estimates, we decided to fit the full model.

Appendix Table B.3. Various spatio-temporal modeling approaches

| | Long-term mean | | | Trend coefficient | | Spatio-temporal residual | | |
|---|---|---|---|---|---|---|---|---|
| Model | Regression | Kriging | Error | Regression | Error | Kriging | Error | Random effect by time |
| Long-term mean and spatio-temporal residuals with spatial correlation | | | | | | | | |
| 1-1 | ■ | ■ | | ■ | | ■ | | |
| 1-2 | ■ | ■ | | ■ | | ■ | | |
| 1-3 | ■ | ■ | | ■ | | ■ | | ■ |
| 1-4 | ■ | ■ | | ■ | | ■ | | ■ |
| 1-5 | ■ | ■ | ■ | ■ | | ■ | | |
| 1-6 | ■ | ■ | ■ | ■ | | ■ | | |
| 1-7 | ■ | ■ | ■ | ■ | | ■ | | ■ |
| 1-8 | ■ | ■ | ■ | ■ | | ■ | | ■ |
| No spatial correlation for long-term mean | | | | | | | | |
| 2-1 | ■ | | ■ | ■ | | ■ | | |
| 2-2 | ■ | | ■ | ■ | | ■ | | |
| 2-3 | ■ | | ■ | ■ | | ■ | | ■ |
| 2-4 | ■ | | ■ | ■ | | ■ | | ■ |
| No spatial correlation for spatio-temporal residuals | | | | | | | | |
| 3-1 | ■ | ■ | | ■ | | | ■ | |
| 3-2 | ■ | ■ | ■ | ■ | | | ■ | |
| 3-3 | ■ | ■ | | ■ | | | ■ | ■ |
| 3-4 | ■ | ■ | ■ | ■ | | | ■ | ■ |
| No spatial correlation for long-term mean and spatio-temporal residuals | | | | | | | | |
| 4-1 | ■ | | ■ | ■ | | | ■ | |

Appendix Table B.4. Selected spatio-temporal models for each $PM_{2.5}$ component by city out of 18 approaches

| City | Pollutant | | | |
|---|---|---|---|---|
| | Sulfur | Silicon | EC | OC |
| LA | 1-2 | 1-3 | 1-2 | 1-2 |
| Chicago | 1-1 | 1-2 | 1-2 | 4-2 |
| Minneapolis-St. Paul | 3-3 | 3-3 | 1-2 | 1-2 |
| Baltimore | 2-2 | 2-2 | 2-2 | 2-2 |
| NY | 2-2 | 1-2 | 3-1 | 1-1 |
| Winston-Salem | 1-2 | 1-2 | 3-3 | 2-1 |

## Estimated regression and variance parameters

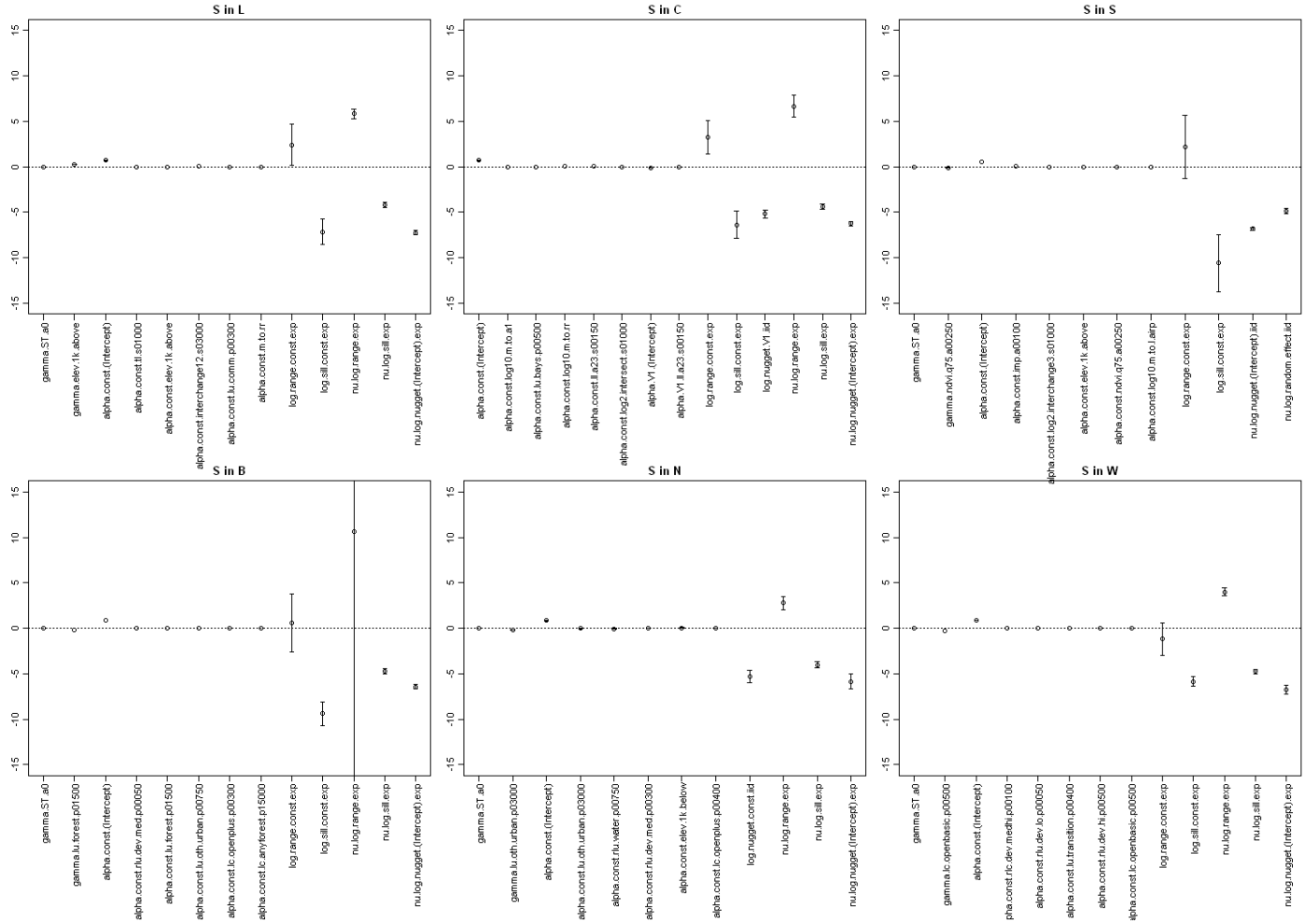


Appendix Figure B.4. Estimated regression and covariance parameters for sulfur in the spatio-temporal model by city

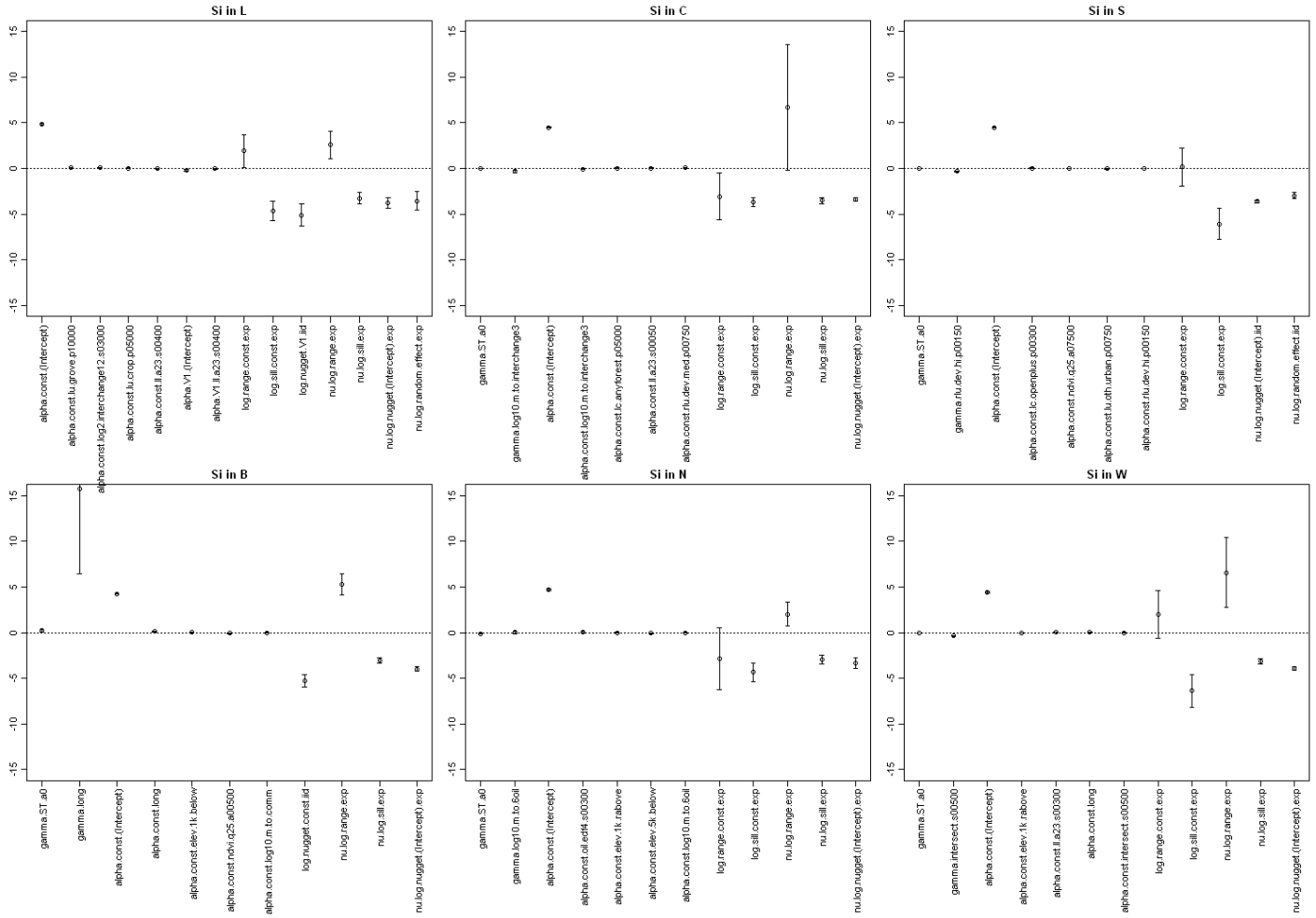


Appendix Figure B.5. Estimated regression and covariance parameters for silicon in the spatio-temporal model by city

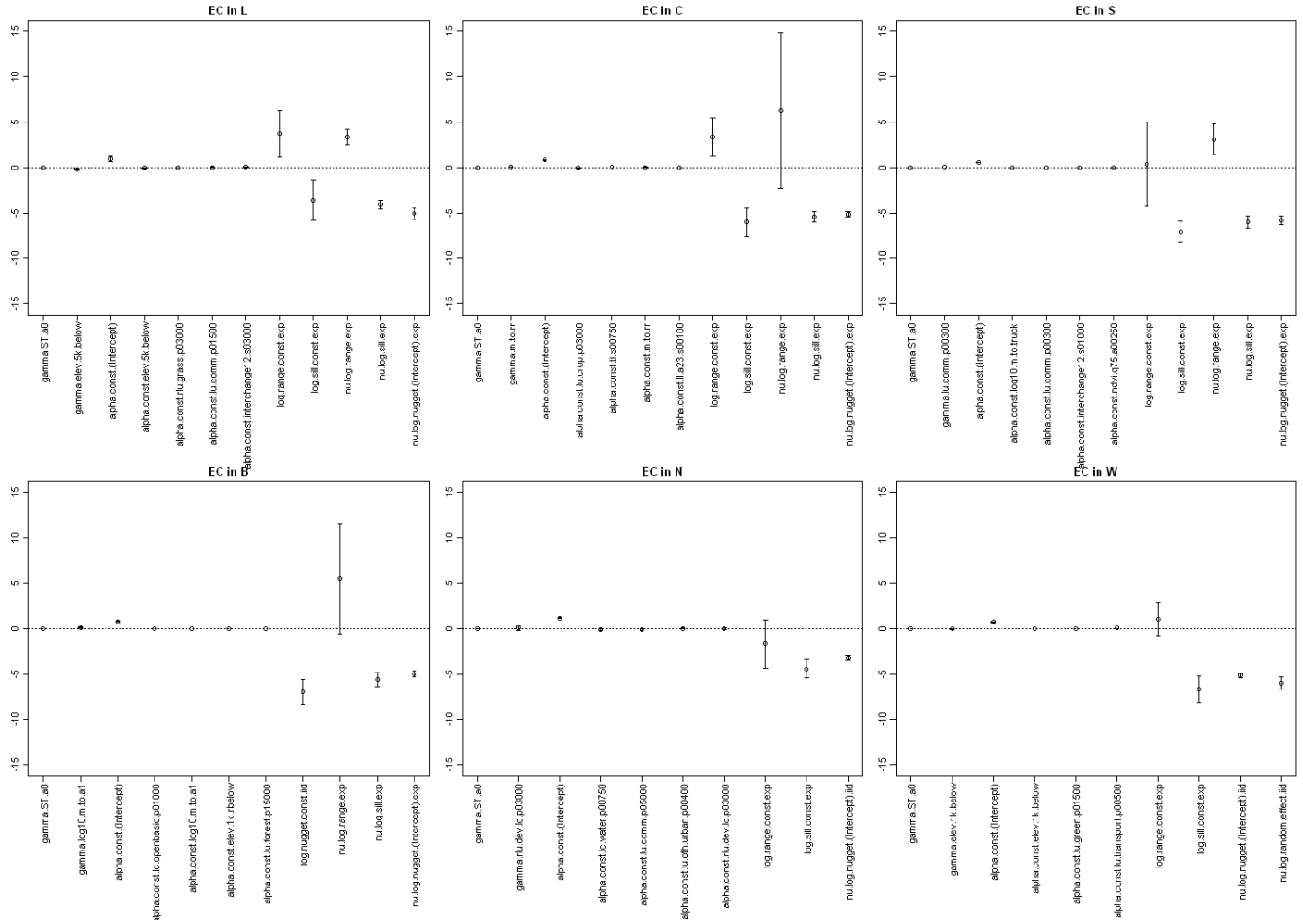


Appendix Figure B.6. Estimated regression and covariance parameters for EC in the spatio-temporal model by city

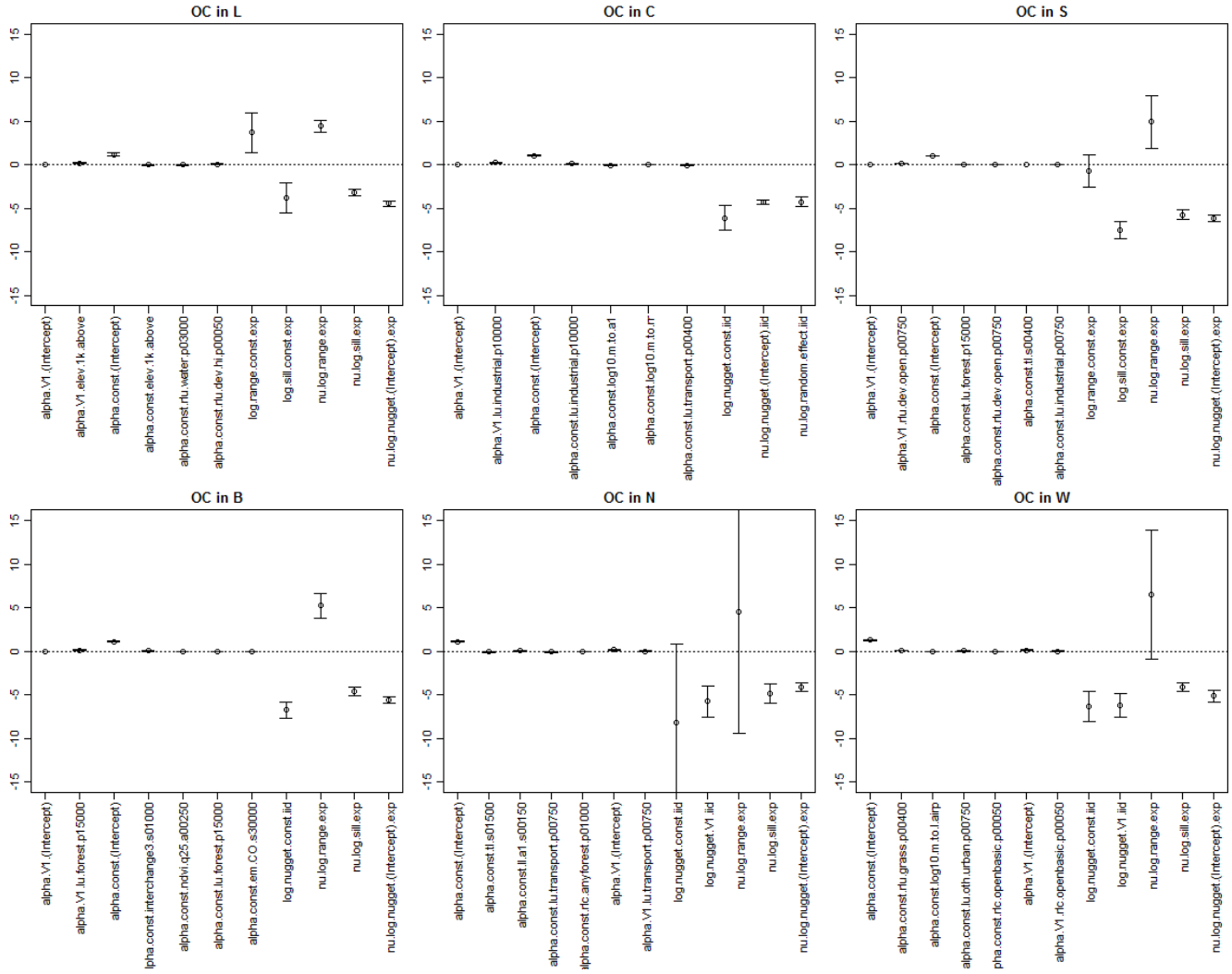


Appendix Figure B.7. Estimated regression and covariance parameters for OC in the spatio-temporal model by city

**Calculation of temporally-adjusted $R^2$**

We attempted to adjust for temporal variability by using $MSE_{REF}$ of 2-week observations centered on a representative temporal trend instead of variance centered on the overall mean in traditional $R^2$. The representative temporal trend was defined by two approaches; the first trend component from singular value decomposition across fixed sites and spatial averages of fixed sites at each time. Temporally-adjusted $R^2$ using the estimated trend was generally higher than those using the spatial averages, particularly for sulfur and silicon (Table 29 in the Section 1 main text). This difference could be because the estimated trend was less representative leading increasing $R^2$ or spatial means computed based on one or two fixed sites at some time points included spatial characteristics in addition to temporal information resulting in decreasing $R^2$. It is not clear which approach provides the temporal trend closer to the true trend. We decided to present both as the main cross-validation result. Below is the mathematical notation for temporally-adjusted $R^2$.

$$\max(0,\ 1-\frac{MSE}{MSE_{REF}}) = \max(0,\ 1-\frac{E(\ (C(s,t)-\hat{C}(s,t))^2)}{E(\ (C(s,t)-\tilde{C}_{fixed}(\cdot,t))^2)}\ )$$